Tunneling density of states and plasmon excitations in double-quantum-well systems

Godfrey Gumbs* and G. R. Aĭzin
Department of Physics and Astronomy, Hunter College of the City University of New York, 695 Park Avenue, New York, New York 10021
(Received 31 October 1994)

We calculate the tunneling density of states and plasmon excitations in a double-quantum-well system. In these calculations, the barriers are doped uniformly. The eigenfunctions are first obtained in the Hartree approximation and these results are then used to calculate the exchange contribution in lowest order. This is a simple way to include the effects due to temperature on the intersubband transition energies. We present a self-consistent-field theory and numerical calculations for the intersubband plasmon excitation energies. The derived analytical results show that in the long wavelength limit the symmetric mode is not affected by tunneling but the antisymmetric mode depends on the charge transfer between the quantum wells. The results for the antisymmetric modes include corrections to previous results where tunneling between the layers was neglected. For the symmetric mode, the sign of the charge density fluctuations in each quantum well is the same and the double-well structure is completely symmetric with respect to the midplane. There is a preferred direction for electrons to tunnel when the charge density fluctuations in the wells have opposite signs which cause the plasmon frequency for the antisymmetric case to depend on tunneling. We also show that in the quasiclassical regime ($q \ll k_{\rm TF}$) there is no minimum separation between the charged layers for the plasmon excitations with wave number q not to be Landau damped. We also examine the effect on the tunneling density of states and the plasmon excitation spectrum when the doping density of the barriers is not the same; specifically, the volume dopant density in the left barrier is larger than the dopant density in the other two barriers, which are assumed to be equally doped.

I. INTRODUCTION AND MOTIVATION

There has long been an interest in double-quantum-well structures[1–3] in both the presence and the absence of an external magnetic field. More recently,[4–19] several papers have been concerned with the electronic properties of these structures. In many of the theoretical calculations reported so far, the electron gas (EG) systems within the quantum wells have been treated as two dimensional (2D). Clearly, this is not an adequate way to treat this problem when one is interested in the plasmon excitations associated with the excitation of an electron between subbands. In the experiments of Ashoori *et al.*[10,11] and Eisenstein *et al.*[14] the 2D EG's occur in GaAs quantum wells which are separated by AlAs tunneling barriers. Typically, the samples used in Refs. 4, 10, 11, and 14 have well widths which are 200 Å and the barrier widths between the wells are from 50 to 150 Å and the confining potential is 250 meV high. Therefore, it seems appropriate to include the coupling between the quantum wells and not treat either well as an isolated 2D EG system. Furthermore, because of the intralayer and interlayer electron-electron interactions and the interlayer tunneling of the electrons, novel properties associated with the intersubband transitions will result, which cannot be explained by a simple single-particle theory due to the role played by the Coulomb correlations. The calculations we carried out for this paper were done in the absence of an external magnetic field. However, there is a body of work on the finite magnetic field effects on double-layer systems, especially in the extreme quantum limit where only the lowest Landau level is occupied. We have extended our zero-field formalism to deal with the density of states (DOS) and plasmon excitations in a perpendicular external magnetic field[20] when the finite width of each quantum well is taken into account and the difference in the effective mass in the quantum wells and the barrier region is included. In this case, the cyclotron frequency is labeled by the quantum number for the envelope functions due to the confinement of electrons in the z direction within the quantum well which leads to discrete energy subbands. These effects, as well as screening within the electron gas, will definitely govern the scaling of the Fermi energy with the magnetic field.[21]

In Ref. 14, the tunneling DOS was measured by capacitance spectroscopy for a magnetic field perpendicular to the plane of the electron gas. The doping of the barrier regions was done so that the electron density in each of the double quantum wells was the same when no interlayer tunneling voltage was applied. In the formal presentation of our theory, we are allowed to have arbitrary doping so that the electron density in the quantum-well layers can be different. We explore the consequences of an imbalance in the electron densities in the two confined systems on the plasmon excitations and the tunneling DOS.

The rest of this paper is organized as follows. In Sec. II, we present the self-consistent Hartree equation and exchange correction to the self-energy for the double-layer quantum system. We include the variation of the effective mass with subband energy and present numerical

0163-1829/95/51(11)/7074(11)/$06.00

results for the electronic wave functions, the conduction band edge showing band-bending effects obtained in the Hartree approximation, the electron effective mass, the subband energy levels, and the DOS. In Sec. III, we use linear response theory to derive the dispersion relation for plasmon excitations. This formalism includes the polarization effects of the medium. Numerical results are presented in Sec. IV for the plasmon excitations. In Sec. V, we summarize our results and use a density matrix approach in the Appendix to identify the symmetry of the modes of excitation given by our dispersion relation in Sec. III.

II. QUASIPARTICLE ENERGY AND THE DENSITY OF STATES

Our method of calculation of the self-energy in the Green's function is based on the dielectric response function formalism of Martin and Schwinger.[22] The general formulation is described as follows. We expand the Green's function in terms of a complete set of states $\phi_{\mathbf{k},n}$ which satisfy the Schrödinger and Poisson equations simultaneously. That is,

$$G(\mathbf{r},\mathbf{r}';\omega)=\sum_{\mathbf{k},n}\phi_{\mathbf{k},n}(\mathbf{r})\phi^{*}_{\mathbf{k},n}(\mathbf{r}')\,G_{\mathbf{k},n}(\omega), \tag{1}$$

$$\phi_{\mathbf{k},n}(\mathbf{r})=\frac{1}{A^{1/2}}e^{i\mathbf{k}\cdot\mathbf{r}_{||}}\zeta_n(k;z), \tag{2}$$

where n is a subband index, $\mathbf{r}=(\mathbf{r}_{||},z)$ is a position vector, $\mathbf{k}$ and $\mathbf{r}_{||}$ are 2D vectors, A is the sample area, and the confinement of an electron in the z direction within the quantum well leads to discrete energy subbands which are self-consistently determined by the Schrödinger equation

$$\left(-\frac{\hbar^2}{2}\frac{d}{dz}\frac{1}{m(z)}\frac{d}{dz}+V_b(z)+\frac{\hbar^2k^2}{2m(z)}+V_H(z)\right)\zeta_n(k;z)$$
$$=\epsilon_{\mathbf{k},n}\zeta_n(k;z)\ , \tag{3}$$

and Poisson's equation for the Hartree potential $V_H(z)$. We solve Eq. (3) perturbatively by solving it for $k=0$ in conjunction with Poisson's equation to obtain the envelope function $\zeta_n(z)\equiv\zeta_n(k=0;z)$ and the subband edge E_n

$$\frac{d}{dz}\varepsilon(z)\frac{d}{dz}V_H(z)=4\pi e^2\left[N_0^{+}(z)-\eta\sum_n\frac{k_BT}{E_{F,n}}|\zeta_n(z)|^2\right.$$
$$\left.\times\ln\left(1+e^{(\mu-E_n)/k_BT}\right)\right]\ , \tag{4}$$

where μ is the chemical potential, $E_{F,n}=\hbar^2(2\pi n_{2D})/2m_n^{*}$, and $\eta=\int_{-\infty}^{\infty}dz\ N_0^{+}(z)$. We calculate the energy dispersion from the zeroth-order wave functions $\zeta_n(z)$ by treating the term $\hbar^2k^2/2m(z)$ in Eq. (3) as a first-order perturbation. We obtain $\epsilon_{\mathbf{k},n}=E_n+\hbar^2k^2/2m_n^{*}$, where the variation of the electron effective mass m_n^{*} in the ground and excited states is included in this treatment. In this perturbation theory approach, the electron effective mass is given by

$$\frac{1}{m_n^{*}}=\int_{-\infty}^{\infty}dz\frac{|\zeta_n(z)|^2}{m(z)}=\frac{p_n}{m_W^{*}}+\frac{1-p_n}{m_B^{*}}\ , \tag{5}$$

where m_W^{*} is the electron effective mass in the well, m_B^{*} is the electron effective mass in the barrier, and p_n is the integral of $|\zeta_n(z)|^2$ over the wells.[23] Clearly, by including the mismatch of the electron effective mass $m(z)$ in the z direction, we obtain an energy-dependent effective mass for the electron subbands, whose wave functions are *not* confined to the quantum-well regions but extend into the barrier regions as well. The variable background dielectric constant is accounted for through $\varepsilon(z)$. These effective masses for the energy subbands are definitely influenced by doping and temperature through the envelope functions $\zeta_n(z)$ determined self-consistently from Eqs. (3) and (4).[24,25] Our numerical calculations show that m_n^{*} increases with the band index.[26] The bare confining potential $V_b(z)$ is taken as zero inside the well and $0.81x$ eV outside, where x is the mole fraction of Al in $GaAs/Al_xGa_{1-x}As$ quantum wells. We take $x=0.32$ in our numerical calculations. In Eq. (4), $N_0^{+}(z)$ is the doping concentration and the integrated total charge on the right-hand side of Eq. (4) is zero by charge neutrality. For a given temperature, the Fermi energy is determined iteratively from the charge neutrality condition. We make the standard assumption that all the donors are ionized even at low temperatures. The doping is taken to be uniform throughout the barrier and the envelope functions are zero at the two ends far away from the interfaces of the quantum well.

The poles of the Green's function expansion coefficients $G_{\mathbf{k},n}(\omega)$ in Eq. (1) are obtained from Dyson's equation. The quasiparticle energies correspond to the solutions of

$$\omega_{\mathbf{k},n}=\omega^{(0)}_{\mathbf{k},n}+\Sigma_{\mathbf{k},n}(\omega_{\mathbf{k},n})\ , \tag{6}$$

where $\hbar\omega^{(0)}_{\mathbf{k},n}=\epsilon_{\mathbf{k},n}-\mu$ and the self-energy is given by

$$\Sigma_{\mathbf{k},n}(\omega)=i\int_{-\infty}^{\infty}\frac{d\omega'}{2\pi}e^{i\omega'0^{+}}\sum_{n'}\int\frac{d^2\mathbf{q}}{(2\pi)^2}G_{\mathbf{k}-\mathbf{q},n'}(\omega')$$
$$\times\int_{-\infty}^{\infty}dz\int_{-\infty}^{\infty}dz'\ \zeta_n(z)\zeta_n(z')\zeta_{n'}(z)\zeta_{n'}(z')$$
$$\times V_{\rm sc}(z,z';\mathbf{q},\omega-\omega')\ . \tag{7}$$

Therefore, many-body and temperature effects contribute to the self-energy through Eq. (7) in conjunction with the equation for the screened potential, which is given by

$$V_{\rm sc}(z,z';\mathbf{q},\omega)=\int_{-\infty}^{\infty}dz''\ \epsilon^{-1}(z,z'';\mathbf{q},\omega)\,v_b(z'',z';q)\ , \tag{8}$$

where the bare Coulomb interaction is $v_b(z,z';q)=$

$2\pi e^2 \exp(-q|z-z'|)/\varepsilon_s q$, with $\varepsilon_s = 4\pi\varepsilon_0\varepsilon_b$ for an average background dielectric constant ε_b. Equations (6)–(8) give the quasiparticle energies with exchange and correlation effects included. However, in this paper, we restrict our numerical calculations to the Hartree and exchange contributions to the quasiparticle energies as a first step in our determination of the role played by the Coulomb interaction on the plasmon excitation energies.

From these results, we obtain the tunneling density of states as

$$\rho(E) = -\frac{1}{\pi}\mathrm{Im}\sum_n \frac{1}{d_x d_y} \times \sum_{\mathbf{k}} \frac{1}{E - E_n - \frac{\hbar^2\mathbf{k}^2}{2m_n^*} - \Sigma_n(\mathbf{k}) + i\hbar/\tau} , \quad (9)$$

where τ is a phenomenological scattering time, $d_x d_y$ is the cross-sectional area of the quantum-well structure, and $\mathbf{k} = 2\pi(n_x/d_x, n_y/d_y)$ with $n_x, n_y = 0, \pm1, \pm2, \ldots$.

III. LINEAR RESPONSE THEORY

In this section, we use linear response theory to obtain the dispersion relation for plasmon excitations in a double-quantum-well structure.

A. Dispersion relation for plasmon excitations

In self-consistent-field theory, the inverse dielectric function is a solution of the integral equation

$$\epsilon^{-1}(z_1, z_2; q, \omega) = \delta(z_1 - z_2) + \int_{-\infty}^{\infty} dz_3 \int_{-\infty}^{\infty} dz_4\, v_b(z_1, z_3; q) \times \chi^0(z_3, z_4; q, \omega)\epsilon^{-1}(z_4, z_2; q, \omega) . \quad (10)$$

Therefore, screening involves polarization effects which are described in terms of the density-density response function $\chi^0(z, z'; q, \omega)$. If exciton binding within an electron-hole pair plays a role, vertex corrections to the polarization function must be included. In the ladder approximation, we have[27,28]

$$\chi^0(z_1, z_2; q, \omega) = \sum_{n,n'} \Pi^{(0)}_{n,n'}(q, \omega)\zeta_n(z_1)\zeta_n(z_2)\zeta_{n'}(z_2)\zeta_{n'}(z_1) , \quad (11)$$

where the polarization function is given by

$$\Pi^{(0)}_{n,n'}(q, \omega) \equiv 2\int \frac{d^2\mathbf{k}}{(2\pi)^2} \frac{f_0(\epsilon_{\mathbf{k},n}) - f_0(\epsilon_{\mathbf{k}-\mathbf{q},n'})}{\hbar\omega + \epsilon_{\mathbf{k},n} - \epsilon_{\mathbf{k}-\mathbf{q},n'} + i\gamma} \times \Gamma_{nn'}(\mathbf{k}, \mathbf{q}; \omega) . \quad (12)$$

Here γ is a parameter due to impurity and phonon scattering, $f_0(\epsilon)$ is the Fermi distribution function,

$$\Gamma_{nn'}(\mathbf{k}, \mathbf{q}; \omega) = 1 + \int \frac{d^2\mathbf{p}}{(2\pi)^2} V^{\mathrm{ex}}_{nn'}(\mathbf{k} - \mathbf{p}) \times \frac{f_0(\epsilon_{\mathbf{p},n}) - f_0(\epsilon_{\mathbf{p}-\mathbf{q},n'})}{\hbar\omega + \epsilon_{\mathbf{p},n} - \epsilon_{\mathbf{p}-\mathbf{q},n'} + i\gamma} \Gamma_{nn'}(\mathbf{p}, \mathbf{q}; \omega) , \quad (13)$$

and $V^{\mathrm{ex}}_{nn'}(\mathbf{k})$ is the static-screened exciton interaction whose screening length depends on the density of states at the Fermi energy of the 2D electron gas. We have[29]

$$V^{\mathrm{ex}}_{nn'}(\mathbf{k} - \mathbf{k}') = -\left(\frac{2\pi e^2}{\varepsilon_s}\right) \frac{F_{nn'}(|\mathbf{k} - \mathbf{k}'|)}{|\mathbf{k} - \mathbf{k}'| + q_s S_{\mathrm{TF}}(|\mathbf{k} - \mathbf{k}'|)} , \quad (14)$$

where the electron screening and subband form factors are defined as

$$S_{\mathrm{TF}}(|\mathbf{k} - \mathbf{k}'|) = \frac{1}{n_{2\mathrm{D}}^2} \int_{-\infty}^{\infty} dz \int_{-\infty}^{\infty} dz' \times e^{-|\mathbf{k}-\mathbf{k}'||z-z'|} n(z)^2, \quad (15)$$

$$F_{nn'}(|\mathbf{k} - \mathbf{k}'|) = \int_{-\infty}^{\infty} dz \int_{-\infty}^{\infty} dz'\, e^{-|\mathbf{k}-\mathbf{k}'||z-z'|} \times |\zeta_n(z)|^2 |\zeta_{n'}(z')|^2 , \quad (16)$$

and q_s is a screening length which depends on the density of states of the 2D electron gas.

The contributions from the many-body and temperature effects to the quasiparticle energies are more clearly identified if closed-form analytic results for the self-energy are obtained. In order to simplify our calculations, we replace the Green's function in Eq. (7) by a Hartree approximation. By setting $\epsilon^{-1}(z - z'; q, \omega) = \delta(z - z')$, we neglect the screening effects which are given by the second term in Eq. (10). Consequently, we obtain the following approximation for the exchange part of the self-energy:

$$\hbar\Sigma^{\mathrm{exch}}_{\mathbf{k},n} = -\sum_{n'} \int \frac{d^2\mathbf{q}}{(2\pi)^2} \times \int_{-\infty}^{\infty} dz \int_{-\infty}^{\infty} dz'\, \zeta_n(z)\zeta_{n'}(z)\zeta_n(z')\zeta_{n'}(z') \times \frac{2\pi e^2}{\varepsilon_s q} e^{-q|z-z'|} f_0(\epsilon_{\mathbf{k}-\mathbf{q},n'}) , \quad (17)$$

which is a generalization of the result of Bandara *et al.*[30] to finite temperature for the correction to the Hartree energy E_n in Eq. (3). Since $\Sigma^{\mathrm{exch}}_{\mathbf{k},n}$ is independent of frequency, the quasiparticle energy is given by a closed-form analytic result. The numerical results presented in this paper were obtained by calculating the integral over the 2D wave vector $\mathbf{q}$ in Eq. (17) exactly[31] and not limiting the calculation to the long wavelength limit $\mathbf{q} \to 0$.

We have solved Eq. (10) for $\epsilon^{-1}(z,z';q,\omega)$ when the Coulomb potential is included and obtained the following analytic result:

$$\epsilon^{-1}(z_1,z_2;q,\omega) = \delta(z_1-z_2) + \sum_{n,n'} \Pi^{(0)}_{nn'}(q,\omega) w_{nn'}(z_1;q) \times K_{nn'}(z_2;q,\omega) \ , \tag{18}$$

where

$$w_{nn'}(z_1;q) \equiv \int_{-\infty}^{\infty} dz_3 \ v_{\rm b}(z_1,z_3;q)\,\zeta_n(z_3)\zeta_{n'}(z_3) \tag{19}$$

and

$$K_{nn'}(z;q,\omega) \equiv \int_{-\infty}^{\infty} dz' \ \zeta_n(z')\zeta_{n'}(z') \ \epsilon^{-1}(z',z;q,\omega) \ . \tag{20}$$

After multiplying Eq. (18) by $\zeta_\alpha(z_1)\zeta_\beta(z_1)$ and integrating over z_1, we obtain

$$\sum_{n,n'} \epsilon_{\alpha\beta;nn'}(q,\omega) K_{nn'}(z;q,\omega) = \zeta_\alpha(z)\ \zeta_\beta(z) \ , \tag{21}$$

where we define the form factored Coulomb potential by

$$u_{mm';nn'}(q) \equiv \int_{-\infty}^{\infty} dz \int_{-\infty}^{\infty} dz' \ \zeta_m(z)\zeta_{m'}(z) v_{\rm b}(z,z';q) \times \zeta_n(z')\zeta_{n'}(z') \tag{22}$$

and the dielectric tensor by

$$\epsilon_{\alpha\beta;nn'}(q,\omega) = \delta_{\alpha n}\delta_{\beta n'} - u_{\alpha\beta;nn'}(q)\Pi^{(0)}_{nn'}(q,\omega). \tag{23}$$

Clearly, the poles of the inverse dielectric function in Eq. (18) correspond to the zeros of the determinant of the dielectric tensor in Eq. (23). Thus we obtain an analytic formula for the plasmon dispersion relation in a double quantum well corresponding to an electronic transition between the subbands as

$$\text{Det}\ \epsilon_{\alpha\beta;nn'}(q,\omega) = 0 \ . \tag{24}$$

The formalism presented here includes the effect due to interband scattering of the electrons and our plasmon dispersion relation in Eq. (24) agrees with the result of Das Sarma and Madhukar[1] (see their Appendix A). In the limit, when the envelope functions $\zeta_n(z)$ for the nth subband describe extremely strong confinement, the overlap of the wave functions can be neglected. Specifically, when only two degenerate subbands are included and we approximate the amplitude of the wave functions by δ functions centered on planes at $z = a_0$ and $z = b_0$, the positions of the 2D EG's within the wells, our results for the symmetric and antisymmetric plasmon excitation energies in the long wavelength limit, agree with Ref. 1. That is, with $|\zeta_1(z)|^2 = \delta(z-a_0)$, $|\zeta_2(z)|^2 = \delta(z-b_0)$, and $2a = |a_0 - b_0|$, Eq. (22) yields

$$\begin{aligned} u_{11;11}(q) &= 2\pi e^2/\varepsilon_s q, \\ u_{11;22}(q) &= 2\pi e^2 \exp(-2qa)/\varepsilon_s q, \end{aligned} \tag{25}$$

which may be used in Eq. (24). We now present closed-form analytic results for the symmetric and antisymmetric modes when tunneling is included, which generalize those of Ref. 1.

B. Analytic results for plasmon excitations with tunneling

We now turn to analytic calculations of the plasmon excitations in a double-well system when the two originally degenerate ground state energy levels in the two wells are split due to tunneling. The higher energy levels will be ignored in these calculations. The width of each well is b with $-a-b < z < -a$ for one quantum well and $a < z < a+b$ for the other quantum well. We shall treat the tunneling as a small perturbation for which the wave functions corresponding to the ground (1) and first excited (2) states can be approximated by

$$\begin{pmatrix} \zeta_1(z) \\ \zeta_2(z) \end{pmatrix} = \frac{1}{\sqrt{2}} \begin{pmatrix} 1 & 1 \\ 1 & -1 \end{pmatrix} \begin{pmatrix} \psi(z-a) \\ \psi(z+a) \end{pmatrix} , \tag{26}$$

where $\psi(z)$ is the ground state wave function of an electron in a single well whose center is at $z = 0$. When the electrons are strongly localized in the wells, we make the approximation that the overlap of the wave functions can be neglected. The two-subband approximation in conjunction with Eq. (26) yields, in the 2D EG limit, the following results for the matrix elements in Eq. (22) when we take $|\psi_n(z)|^2 = \delta(z)$ $(n = 1,2)$:

$$\begin{aligned} u_{11;11} &= u_{11;22} = u_{22;11} = u_{22;22} \\ &= 2\pi e^2 \left(1 + e^{-2qa}\right)/(\varepsilon_s q) \equiv V_1, \\ u_{12;11} &= u_{12;22} = u_{21;11} = u_{21;22} = u_{11;12} \\ &= u_{22;12} = u_{11;21} = u_{22;21} = 0, \\ u_{12;12} &= u_{21;21} = u_{21;12} = u_{12;21} \\ &= 2\pi e^2 \left(1 - e^{-2qa}\right)/(\varepsilon_s q) \equiv V_2. \end{aligned} \tag{27}$$

Making use of Eqs. (27) in Eq. (23), we obtain the dielectric tensor for the two-band model as

$$\begin{pmatrix} \epsilon_{11;11} & \epsilon_{11;12} & \epsilon_{11;21} & \epsilon_{11;22} \\ \epsilon_{12;11} & \epsilon_{12;12} & \epsilon_{12;21} & \epsilon_{12;22} \\ \epsilon_{21;11} & \epsilon_{21;12} & \epsilon_{21;21} & \epsilon_{21;22} \\ \epsilon_{22;11} & \epsilon_{22;12} & \epsilon_{22;21} & \epsilon_{22;22} \end{pmatrix} = \begin{pmatrix} 1-V_1\Pi^{(0)}_{11} & 0 & 0 & -V_1\Pi^{(0)}_{22} \\ 0 & 1-V_2\Pi^{(0)}_{12} & -V_2\Pi^{(0)}_{21} & 0 \\ 0 & -V_2\Pi^{(0)}_{12} & 1-V_2\Pi^{(0)}_{21} & 0 \\ -V_1\Pi^{(0)}_{11} & 0 & 0 & 1-V_1\Pi^{(0)}_{22} \end{pmatrix} . \tag{28}$$

In a straightforward way, it can be shown that the zeros of the dielectric tensor in Eq. (28) are given by the solutions of the two equations

$$V_1(q)\left[\Pi_{11}^{(0)}(q,\omega)+\Pi_{22}^{(0)}(q,\omega)\right]=1,$$
$$V_2(q)\left[\Pi_{21}^{(0)}(q,\omega)+\Pi_{12}^{(0)}(q,\omega)\right]=1, \tag{29}$$

which describe the symmetric and antisymmetric modes of oscillations for the double-layer structure. Equation (29) is similar to the dispersion relation for single quantum wells derived in Ref. 32. To identify which one of these equations describes symmetric plasmon modes and which antisymmetric modes, we refer to the Appendix.

When the difference in the effective mass (m_1^*) for the ground subband and the first excited state (m_2^*) is negligible and vertex corrections are neglected, the polarization functions are given by the formulas

$$\Pi_{11}^{(0)}(q,\omega)=-\frac{m^*}{\pi\hbar^2}\left[1+\frac{m^*}{\hbar q^2}\left\{\sqrt{\left(\omega-\frac{\hbar q^2}{2m^*}\right)^2-q^2v_{F1}^2}-\sqrt{\left(\omega+\frac{\hbar q^2}{2m^*}\right)^2-q^2v_{F1}^2}\right\}\right], \tag{30}$$

$$\Pi_{22}^{(0)}(q,\omega)=-\frac{m^*}{\pi\hbar^2}\left[1+\frac{m^*}{\hbar q^2}\left\{\sqrt{\left(\omega-\frac{\hbar q^2}{2m^*}\right)^2-q^2v_{F2}^2}-\sqrt{\left(\omega+\frac{\hbar q^2}{2m^*}\right)^2-q^2v_{F2}^2}\right\}\right], \tag{31}$$

$$\Pi_{12}^{(0)}(q,\omega)=-\frac{m^*}{\pi\hbar^2}\left[1+\frac{m^*}{\hbar q^2}\left\{\sqrt{\left(\omega+\Delta\Omega-\frac{\hbar q^2}{2m^*}\right)^2-q^2v_{F2}^2}-\sqrt{\left(\omega+\Delta\Omega+\frac{\hbar q^2}{2m^*}\right)^2-q^2v_{F1}^2}\right\}\right], \tag{32}$$

$$\Pi_{21}^{(0)}(q,\omega)=-\frac{m^*}{\pi\hbar^2}\left[1+\frac{m^*}{\hbar q^2}\left\{\sqrt{\left(\omega-\Delta\Omega-\frac{\hbar q^2}{2m^*}\right)^2-q^2v_{F1}^2}-\sqrt{\left(\omega-\Delta\Omega+\frac{\hbar q^2}{2m^*}\right)^2-q^2v_{F2}^2}\right\}\right], \tag{33}$$

where v_{F1} and v_{F2} are the Fermi velocities for the subbands 1 and 2, respectively, and $\Delta\Omega=(E_2-E_1)/\hbar$. Equations (30) and (31) are valid when $\omega>\hbar q^2/2m^*$. Also, in deriving Eqs. (32) and (33), we assumed that $\omega>\Delta\Omega+\hbar q^2/2m$. The results in Eqs. (30)–(33) can be further simplified in the *quasiclassical* approximation when $q\ll k_F$ and $\hbar\omega\ll\epsilon_F$ and we have

$$\Pi_{11}^{(0)}(q,\omega)\approx-\frac{m^*}{\pi\hbar^2}\left[1-\frac{\omega}{\sqrt{\omega^2-q^2v_{F1}^2}}\right], \tag{34}$$

$$\Pi_{22}^{(0)}(q,\omega)\approx-\frac{m^*}{\pi\hbar^2}\left[1-\frac{\omega}{\sqrt{\omega^2-q^2v_{F2}^2}}\right], \tag{35}$$

$$\Pi_{12}^{(0)}(q,\omega)\approx-\frac{m^*}{\pi\hbar^2}\left[1-\frac{\omega}{\sqrt{(\omega+\Delta\Omega)^2-q^2\left(v_{F1}^2+v_{F2}^2\right)/2}}\right], \tag{36}$$

$$\Pi_{21}^{(0)}(q,\omega)\approx-\frac{m^*}{\pi\hbar^2}\left[1-\frac{\omega}{\sqrt{(\omega-\Delta\Omega)^2-q^2\left(v_{F1}^2+v_{F2}^2\right)/2}}\right]. \tag{37}$$

Substituting Eqs. (34) and (35) into Eq. (29), we have shown that the symmetric modes are not affected by tunneling and, in the *quasiclassical* approximation, their normal mode frequencies are given by

$$-\frac{\pi e^2}{\varepsilon_s q}\left(1+e^{-2qa}\right)\frac{m^*}{\pi\hbar^2}\left[2-\frac{\omega}{\sqrt{\omega^2-q^2v_{F1}^2}}-\frac{\omega}{\sqrt{\omega^2-q^2v_{F2}^2}}\right]=1\,. \quad (38)$$

If we make use of $\hbar\Delta\Omega \ll \epsilon_F$, we can take $v_{F1} \approx v_{F2} \approx v_F$; then

$$\omega_+ = \frac{Q_+}{\sqrt{Q_+^2-1}}qv_F, \quad (39)$$

where

$$Q_\pm(q) \equiv 1+\frac{q}{k_{\rm TF}\left(1\pm e^{-2qa}\right)} \quad (40)$$

in terms of the Thomas-Fermi wave number $k_{\rm TF} = 2m^*e^2/\varepsilon_s\hbar^2$. In the long wavelength limit ($q \ll k_{\rm TF}$), Eq. (39) becomes

$$\omega_+^2 = \frac{2\pi n_s e^2}{m^*}q\left(1+e^{-2qa}\right), \quad (41)$$

where n_s is the total electron density. This result may also be obtained directly from Eq. (38) when $qv_{F1,2} \ll \omega$. Equation (41) agrees with the result of Das Sarma and Madhukar[1] for $v_{F1} = v_{F2}$ and with the same electron effective mass in the two quantum wells.

Turning now to the antisymmetric modes, we obtain from Eq. (29) in the quasiclassical limit

$$-\frac{\pi e^2}{\varepsilon_s q}\left(1-e^{-2qa}\right)\frac{m^*}{\pi\hbar^2}\left[2-\frac{\omega}{\sqrt{(\omega+\Delta\Omega)^2-q^2\bar{v}_F^2}}-\frac{\omega}{\sqrt{(\omega-\Delta\Omega)^2-q^2\bar{v}_F^2}}\right]=1, \quad (42)$$

where $\bar{v}_F^2 \equiv (v_{F1}^2+v_{F2}^2)/2$. Clearly, the solution of Eq. (42) depends on tunneling. In the limit $\Delta\Omega \ll q\bar{v}_F$, Eq. (42) yields the result

$$\omega_-^2 = \frac{Q_-^2}{Q_-^2-1}\left(q\bar{v}_F\right)^2+\frac{Q_-^2\left[3Q_-^2-1\right]}{Q_-^2-1}\Delta\Omega^2\,, \quad (43)$$

where Q_- is defined in Eq. (40). Equation (43) reduces to the frequency of oscillation for the antisymmetric mode in the absence of tunneling ($\Delta\Omega \to 0$) that was given by Das Sarma and Madhukar[1] for $q \ll k_{\rm TF}$.

Our result that the symmetric mode is not affected by tunneling but the antisymmetric mode depends on the charge transfer between the wells can be explained as follows. For the symmetric mode, the sign of the charge density fluctuations in each quantum well is the same (see the Appendix) and the double-well structure is completely symmetric with respect to the midplane at $z = 0$. As a consequence, the probability for an electron to tunnel from the well on the right-hand side to the one on the left-hand side and vice versa will be same, thereby causing tunneling to have no effect on the symmetric mode. On the other hand, there is a preferred direction for electrons to tunnel when the charge density fluctuations in the wells have opposite signs, which would definitely impact on the plasmon frequency for this case.

There are two points we would like to discuss before presenting our numerical calculations in Sec. IV. The first concerns the use of the δ-function approximation for the amplitude of the wave functions. Results similar to the dispersion relations in Eq. (29) have been obtained for finite well width with no overlap of the wave functions for electrons in different wells. However, an advantage of taking the $b \to 0$ limit is that in the plasmon dispersion relations, we used the quasiclassical approximation $q \ll k_F$ and $\hbar\omega \ll \epsilon_F$. If both energy levels are occupied, then $k_F b \sim 1$ so that $qb \ll 1$. In this long wavelength limit, the results for the dispersion relations when b is finite are the same as those for the δ-function approximation.

The second point has to do with a result of Das Sarma and Madhukar[1] that the separation between the wells must exceed a certain critical value, otherwise the plasmons are Landau damped. Their calculations were based on a model consisting of degenerate energy levels in the two quantum wells with no tunneling between them ($\Delta\Omega = 0$). When only the two ground degenerate energy levels in the two wells are included, the dispersion relation for plasmon excitations is given by the determinantal equation

$$\begin{vmatrix} 1-u_{11;11}\Pi_{11}^{(0)} & -u_{11;22}\Pi_{22}^{(0)} \\ -u_{11;22}\Pi_{11}^{(0)} & 1-u_{11;11}\Pi_{22}^{(0)} \end{vmatrix} = 0\,, \quad (44)$$

where $u_{11;11}$ and $u_{11;22}$ are given in Eq. (25). As a special case of the dispersion relation in Eq. (44), we take the Fermi velocities to be equal $v_{F1} = v_{F2}$ so that the polarizability functions in Eqs. (30)–(33) are the same. Equation (44) then becomes

$$\left[1-\left(u_{11;11}+u_{11;22}\right)\Pi_{11}^{(0)}\right]\left[1-\left(u_{11;11}-u_{11;22}\right)\Pi_{11}^{(0)}\right] = 0\,. \quad (45)$$

When the result in the first (second) set of square brackets in Eq. (45) is zero, we obtain the dispersion relation for the symmetric (antisymmetric) plasmon excitation modes. In the quasiclassical approximation, Eq. (45) yields, in conjunction with any one of the results for the polarization functions in Eqs. (34)–(37), when $v_{F1} = v_{F2}$ and $\Delta\Omega = 0$, the plasmon excitation energies for the symmetric (+) and antisymmetric (−) mode

$$\omega_\pm = \frac{Q_\pm}{\sqrt{Q_\pm^2-1}}qv_F. \quad (46)$$

Equation (46) clearly shows that $\omega_\pm > qv_F$ so that there

is *no Landau damping* for either mode for any value of the well separation $2a$ in the quasiclassical regime. Therefore, the conclusion by Das Sarma and Madhukar[1] that the separation between the charged layers must exceed some specific critical value if the plasmons are not to be Landau damped is not correct. This result in Ref. 1 was obtained when $\omega \gg qv_F$, which they referred to as the high-frequency limit. This corresponds to $q \ll k_{\rm TF}$ in Eq. (46), which becomes

$$\omega_{\pm} \approx \sqrt{\frac{k_{\rm TF}\,(1 \pm e^{-2qa})}{2q}}\,qv_F\ . \tag{47}$$

After this, the limit $2qa \ll 1$ was taken in Eq. (47) so that the antisymmetric mode frequency becomes $\omega_- \approx (k_{\rm TF}a)^{1/2}\,qv_F$ on which was imposed the condition that $a > 1/k_{\rm TF}$ if this mode is not to be Landau damped.

IV. NUMERICAL RESULTS AND DISCUSSION

In our numerical calculations, we choose a temperature of $T = 50$ K, assume that the entire structure is charge neutral, use infinite barrier boundary conditions, and completely symmetrize the second derivative terms in solving Eqs. (3) and (4). We choose an electron effective mass for the bulk material making up the barrier region and the well region as $m_B = 0.08m_e$ and $m_W = 0.67m_e$, respectively, where m_e is the free-electron mass. The bare confining potential $V_b(z)$ is taken as zero inside the well and 0.26 eV outside. Also, the background dielectric constant for the barrier region and well region is chosen as 12.0 and 13.0, respectively. The width of each barrier is 100 Å and the quantum-well width is 75 Å. In Figs. 1 and 2, we show plots of the conduction band edge and the lowest four electron wave functions when the doping in each of the barriers has a volume density of 20.0×10^{17} cm^{-3}; we assume that all donors are ionized. For this, the total volume density of the dopant charge is 12.0×10^{12} cm^{-2}, the chemical potential is $\mu = 0.345$ eV, and the Fermi wave number is $k_F = 0.0614$ Å^{-1}. The conduction band edge shows band-bending effects obtained by solving the Hartree equation (3) in conjunction with Poisson's equation (4). Figure 3 shows a plot of the averaged (reciprocal) subband effective mass m_n^* defined in Eq. (5) as a function of the subband index n, while Fig. 4 is a plot of the corresponding subband edge E_n^0 and the chemical potential μ. Only four sub-

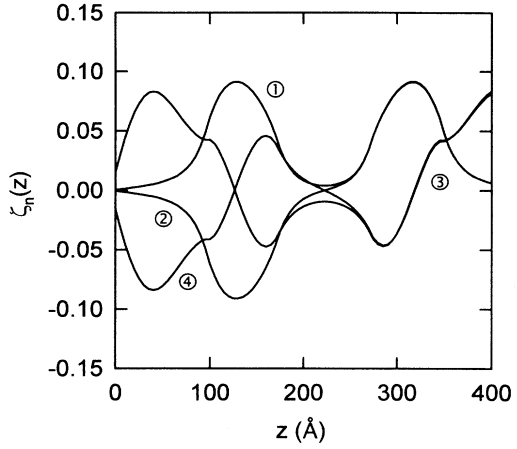

FIG. 2. Electron wave functions of the lowest three single-particle eigenstates calculated in the self-consistent Hartree approximation using Eqs. (3) and (4). These wave functions correspond to the conduction band edge in Fig. 1.

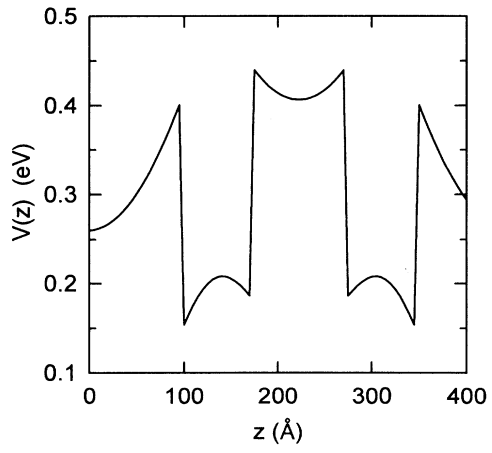

FIG. 1. Conduction band edge of the double-layer quantum-well system. The single-particle eigenstates are calculated in the self-consistent Hartree approximation using Eqs. (3) and (4). The following parameters are chosen: the well width is $L_z = 75$ Å, the dopant density in each barrier region is 20.0×10^{17} cm^{-3}, and the electron effective mass in the well and barrier regions is $m^* = 0.067m_e$ and $m^* = 0.08m_e$, respectively.

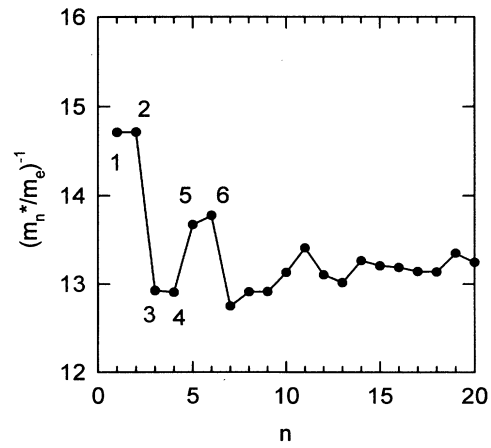

FIG. 3. Averaged reciprocal electron effective mass $1/m_n^*$ in units of the free-electron mass m_e as a function of the subband index n, for the modulation doping used in calculating the results in Figs. 1 and 2. The lowest six electron effective masses are labeled by their indices.

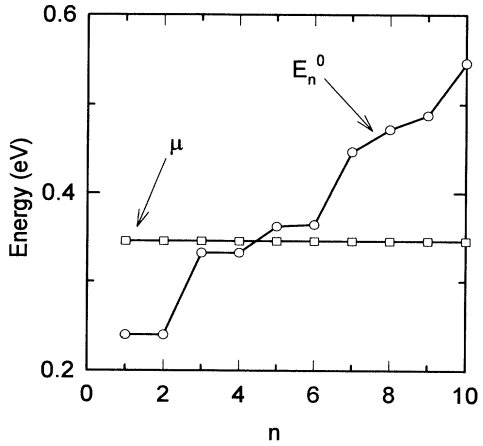

FIG. 4. Conduction band edge E_n^0 (○) and the chemical potential μ (□) for the modulation doping used in calculating the results in Figs. 1–3. For convenience, solid lines are used to connect these points.

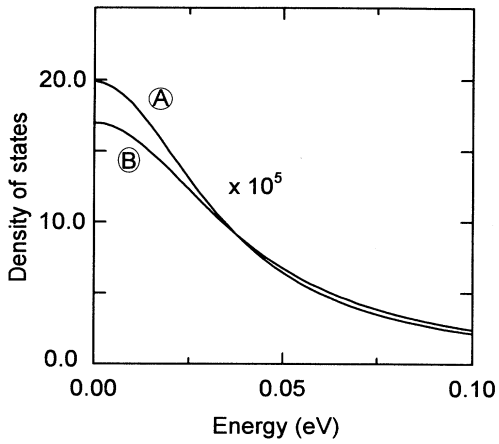

FIG. 6. Tunneling density of states as a function of energy for the double-layer quantum-well system. Curve A is for barrier doping with volume density 20.0×10^{17} cm^{-3} and assuming all donors are ionized. Curve B corresponds to a volume dopant density in the left barrier of 30.0×10^{17} cm^{-3}, but the dopant density in the middle and right-hand barriers is unchanged as 20.0×10^{17} cm^{-3}.

band edges lie below the chemical potential. The original degenerate subband energies are split by tunneling. For example, the two lowest and next two lowest subband edges only have an energy difference of about 0.1 meV, but this difference increases for the higher lying subbands. In Fig. 5, we present the wave functions for the ground and first two excited states when the volume dopant density in the left barrier is increased to 30.0×10^{17} cm^{-3}, but the dopant density in the other two barriers is unchanged as 20.0×10^{17} cm^{-3}. All other parameters in the calculations are the same. In this case, the chemical potential is $\mu = 0.405$ eV. When the structure is asymmetrically doped the splitting between the ground states is about 12 meV. In Fig. 6, the tunneling density of states is plotted as a function of the energy for

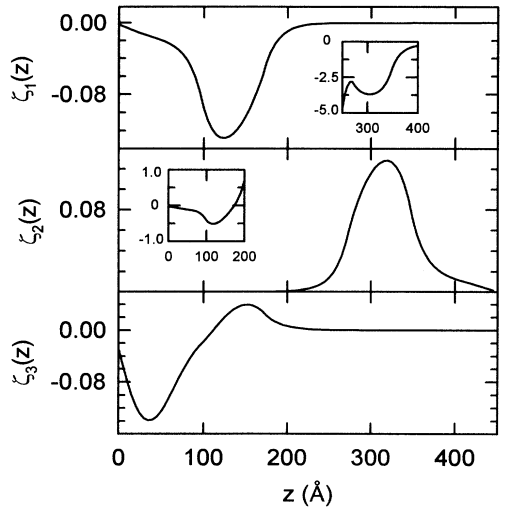

FIG. 5. Electron wave functions of the lowest three single-particle eigenstates calculated in the self-consistent Hartree approximation using Eqs. (3) and (4). These wave functions were calculated when the barrier regions were asymmetrically doped with a dopant volume density of 30.0×10^{17} cm^{-3} within the barrier on the left and 20.0×10^{17} cm^{-3} within the middle barrier and the barrier on the right. The inset shows $\zeta_1(z) \times 10^{-4}$ and $\zeta_2(z) \times 10^{-3}$.

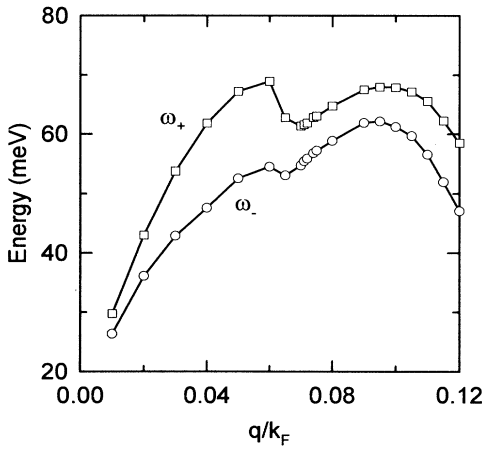

FIG. 7. Plasmon excitation spectrum as a function of the wave vector q in units of the Fermi wave vector $k_F = 6.14 \times 10^{-2}$ Å^{-1} for the double-layer quantum-well system. Here ω_+ is the excitation energy of the symmetric mode and ω_- the excitation energy of the antisymmetric mode. Only the ground and first excited subbands were included in these calculations. The well width is $L_z = 75$ Å, the dopant density in each barrier region is 20.0×10^{17} cm^{-3}, and the electron effective mass in the well and barrier regions is $m^* = 0.067m_e$ and $m^* = 0.08m_e$, respectively.

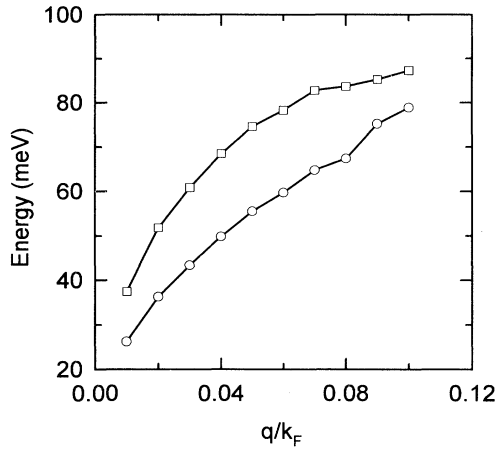

FIG. 8. Plasmon excitation spectrum as a function of the wave vector q in units of the Fermi wave vector $k_F = 6.63 \times 10^{-2}$ Å^{-1} for the double-layer quantum-well system, asymmetrically doped in the barriers only. Only the ground and first excited subbands were included in these calculations. The well width is $L_z = 75$ Å, and the dopant density in the left barrier is 30.0×10^{17} cm^{-3}, but the barrier between the wells and the right-hand barrier have a volume doping density of 20.0×10^{17} cm^{-3}. The electron effective mass in the well and barrier regions is $m^* = 0.067m_e$ and $m^* = 0.08m_e$, respectively.

the double-layer quantum-well system. Curve A is for the case when the doping in each of the barriers has a volume density of 20.0×10^{17} cm^{-3} and all donors are ionized. Curve B corresponds to a volume dopant density in the left barrier of 30.0×10^{17} cm^{-3}, but the dopant density in the other two barriers is unchanged as 20.0×10^{17} cm^{-3}. In Fig. 7, we plot the plasmon excitation spectrum as a function of the wave vector q in units of the Fermi wave vector $k_F = 6.14 \times 10^{-2}$ Å^{-1} for the double-layer quantum-well system. Here both the symmetric (ω_+) and the antisymmetric mode (ω_-) show some structure associated with the difference in the Fermi velocities for the two subbands. Only the ground and first excited subbands were included in these calculations. The well width is $L_z = 75$ Å, the dopant density in each barrier region is 20.0×10^{17} cm^{-3}, and the electron effective mass in the well and barrier regions is $m^* = 0.067m_e$ and $m^* = 0.08m_e$, respectively. Also, we choose the parameter due to impurity and phonon scattering as $\gamma = 0.01\mu$ in the polarization function $\Pi^{(0)}_{n,n'}(q,\omega)$ given by Eq. (12). We compare the results in Fig. 7 with Fig. 8 where the doping in each of the barrier regions is not the same. The volume dopant density in the left barrier is chosen as 30.0×10^{17} cm^{-3}, but the dopant density in the other two barriers is unchanged as 20.0×10^{17} cm^{-3}. All other parameters in the calculations are the same as in Fig. 7. In this case the dip in the plasmon excitation curve occurs at a larger value of the dimensionless wave number. The Coulomb repulsion between the electrons in the two wells and the tunneling cause the originally degenerate modes to be significantly affected in Fig. 7. In Fig. 8 where the energy levels are displaced due to the asymmetry in doping, the weaker tunneling causes the two modes not to have as large a dip as in Fig. 7.

V. CONCLUDING REMARKS AND SUMMARY

In this paper, we presented a self-consistent field theory to calculate the electron wave functions in the Hartree approximation for a double-quantum-well structure. The exchange contribution to the quasiparticle energy was obtained by making use of the Hartree wave functions. Our formalism allows for arbitrary doping of the barrier regions and we assume that all the donors are completely ionized. In our numerical calculations, the doping is taken to be uniform throughout the barrier and the envelope functions are zero at the two ends far away from the interfaces of the quantum well. Our numerical results show that when the barriers are unevenly doped, the built-in electric field causes the electrons to be more localized in one of the wells and the region of localization depends on the subband index (see Fig. 5). This asymmetry of the wave functions has an effect on the plasmon excitation spectrum which we demonstrate in Figs. 7 and 8. Also, we have presented closed-form analytic results for the plasmon excitation spectrum in the long wavelength limit. Our results show that tunneling does not affect the frequency of the symmetric mode, but the contribution due to tunneling on the antisymmetric mode is calculated explicitly. Das Sarma and Madhukar[1] have concluded from their calculations done in the quasiclassical limit that the separation between the wells must exceed a certain critical value, otherwise the plasmons are Landau damped. Their calculations were based on a model consisting of degenerate energy levels in the two quantum wells with no tunneling between them. Equation (46) clearly shows that there is no Landau damping for either the symmetric or antisymmetric mode for any value of the well separation $2a$. Specifically, it follows from Eq. (39) that the symmetric mode will not be Landau damped in the quasiclassical limit ($q \ll k_F$). At small values of q ($q \ll k_{\rm TF}, a$), we have $\omega \sim q$. At large values of q ($k_{\rm TF}, a \ll q \ll k_F$), ω_+ asymptotically approaches the boundary of single-particle excitations ($\omega \to qv_F$) as q increases so that there is Landau damping of ω_+ outside the quasiclassical region. The limiting behavior of the antisymmetric mode is more complex. As a matter of fact, this mode may be considered as an intersubband plasmon excitation between the lowest symmetric and the next antisymmetric level in double quantum wells.[8] It follows from Eq. (42) that as $q \to 0$, $\omega_-^2 \to (1 + 2k_{\rm TF}a)\,\Delta\Omega^2$. Therefore, the deviation of ω_- from the subband spacing $\Delta\Omega$ is produced by depolarization fields similar to intersubband plasmons in single quantum wells.[32] As q increases, the antisymmetric mode approaches the linear dispersion when $q \gg k_{\rm TF}$ and we have $\omega > qv_{\rm F}$. That is, this mode will also not be Landau damped in the quasiclassical region. As a matter of fact, the Landau damping of this mode begins when the ω_- curve crosses the boundary of the single-particle excitations associated with transitions from the ground to the first excited level, i.e., $\omega = \Delta\Omega + qv_F$.

ACKNOWLEDGMENT

The authors acknowledge the support in part from the City University of New York PSC-CUNY Grant No. 664279.

APPENDIX

In this appendix, we show that Eq. (29) describes symmetric and antisymmetric modes for a double-quantum-well system. The density matrix can be written as

$$\rho_S(\mathbf{r}_{||},z,\mathbf{r}'_{||},z';t)=\sum_{\alpha,\alpha'}\sum_{\mathbf{k},\mathbf{k}'}|\alpha;\mathbf{k}\rangle f_{\alpha,\mathbf{k};\alpha',\mathbf{k}'}(t)\langle\alpha';\mathbf{k}'|\ , \tag{A1}$$

where $\mathbf{r}_{||}$ is a 2D vector, $\mathbf{k}=(k_x,k_y)$ $f_{\alpha,\mathbf{k};\alpha',\mathbf{k}'}(t)$ is the probability of the system to make a transition from the state $|\alpha;\mathbf{k}\rangle$ to the state $|\alpha';k'_x,k'_y\rangle$ at time t. In the absence of the external perturbation, the value of ρ_S in equilibrium is

$$\begin{aligned}\rho_0(\mathbf{r}_{||},z,\mathbf{r}'_{||},z')&\equiv\rho_S(\mathbf{r}_{||},z,\mathbf{r}'_{||},z';t=-\infty)\\&=2\sum_{\alpha,\mathbf{k}}|\alpha;\mathbf{k}\rangle f_0(\epsilon_{\alpha,\mathbf{k}})\langle\alpha;\mathbf{k}|\ ,\end{aligned} \tag{A2}$$

where $f_0(\epsilon_{\alpha,\mathbf{k}})=1/\{\exp[(\epsilon_{\alpha,\mathbf{k}}-\mu)/k_BT]+1\}$ is the Fermi distribution function. Now we consider a system close to thermal equilibrium, perturbed by an external force. We assume that the external force is weak enough so that the difference between the expectation value of any physical quantity and its equilibrium value is *linear* in the force. In this case, the equation of motion of the density matrix in Eq. (A1) is linearized by setting $\rho_S=\rho_0+\rho_1$ and the total Hamiltonian $H=H_0+H_1$, where $H_1(\mathbf{r}_{||},z;t)$ represents the perturbation part of the Hamiltonian due to both the external electric field and the induced density. Keeping only first-order terms, we have

$$i\hbar\frac{\partial\rho_1}{\partial t}\approx[H_1,\rho_0]+[H_0,\rho_1]. \tag{A3}$$

For a periodic force with $H_1(\mathbf{r}_{||},z;t)=H_1(\mathbf{r}_{||},z;\omega)\exp[-i(\omega+i/\tau)t]$ and $\rho_1(\mathbf{r}_{||},z,\mathbf{r}'_{||},z';t)=\rho_1(\mathbf{r}_{||},z,\mathbf{r}'_{||},z';\omega)\exp[-i(\omega+i/\tau)t]$, with τ denoting a phenomenological optical broadening parameter from impurity scattering, we obtain the matrix elements of the perturbed density matrix from Eq. (A3) as

$$\begin{aligned}&\langle\alpha;\mathbf{k}|\rho_1(\mathbf{r}_{||},z,\mathbf{r}'_{||},z';\omega)|\alpha';\mathbf{k}'\rangle\\&\quad=\Pi_{\alpha,\mathbf{k};\alpha',\mathbf{k}'}(\omega)\langle\alpha;\mathbf{k}|H_1|\alpha';\mathbf{k}'\rangle,\end{aligned} \tag{A4}$$

where

$$\Pi_{\alpha,\mathbf{k};\alpha',\mathbf{k}'}(\omega)=2\frac{f_0(\epsilon_{\alpha,\mathbf{k}})-f_0(\epsilon_{\alpha',\mathbf{k}'})}{\hbar\omega-[\epsilon_{\alpha',\mathbf{k}'}-\epsilon_{\alpha,\mathbf{k}}]+i\hbar/\tau}\ . \tag{A5}$$

In the random-phase approximation, the perturbed part of the Hamiltonian is separated into two terms consisting of the external and induced potentials due to density fluctuations so that $H_1(\mathbf{r}_{||},z;\omega)=-e\left[\varphi^{\rm ext}(\mathbf{r}_{||},z)+\Phi^{\rm ind}(\mathbf{r}_{||},z;\omega)\right]$, where $\Phi^{\rm ind}$ is a solution of Poisson's equation

$$\begin{aligned}&\frac{\partial^2\Phi^{\rm ind}(q,z;\omega)}{\partial z^2}-q^2\Phi^{\rm ind}(q,z;\omega)\\&\quad=\frac{4\pi e}{\epsilon_s}\sum_{\alpha,\alpha'}\delta f_{\alpha,\alpha'}(q,\omega)\zeta_\alpha(z)\zeta_{\alpha'}(z)\ .\end{aligned} \tag{A6}$$

Here $\delta f_{\alpha\alpha'}(q,\omega)$ is equal to the sum over $\mathbf{k}$ of $\langle\alpha;\mathbf{k}|\rho_1(\mathbf{r}_{||},z,\mathbf{r}'_{||},z';\omega)|\alpha';\mathbf{k}-\mathbf{q}\rangle$. The envelope function in the z direction is $\zeta_\alpha(z)$. Equation (A4) can be expressed as

$$\delta f_{\alpha\alpha'}(q,\omega)=-e\ \left[\varphi^{\rm ext}_{\alpha\alpha'}(q)+\Phi_{\alpha\alpha'}(q,\omega)\right]\Pi^{(0)}_{\alpha\alpha'}(q,\omega)\ , \tag{A7}$$

where $\Pi^{(0)}_{\alpha\alpha'}$ is the polarization operator defined in Eq. (12) and

$$\Phi_{\alpha\alpha'}(q,\omega)\equiv\int_{-\infty}^{\infty}dz\ \zeta_\alpha(z)\Phi^{\rm ind}(q,z;\omega)\zeta_{\alpha'}(z). \tag{A8}$$

We now solve Eq. (A6) when only the two lowest tunneling states are included in the calculation and the overlap of these wave functions is neglected. For this, the envelope functions are given by Eq. (26). In the extreme case when $|\psi(z)|^2$ is approximated by $\delta(z)$, Eq. (A6) becomes

$$\begin{aligned}&\frac{\partial^2\Phi^{\rm ind}(q,z;\omega)}{\partial z^2}-q^2\Phi^{\rm ind}(q,z;\omega)\\&\quad=\frac{2\pi e\delta}{\epsilon_s}F_1\ \delta(z-a)+\frac{2\pi e\delta}{\epsilon_s}F_2\ \delta(z+a)\ ,\end{aligned} \tag{A9}$$

where $\delta F_1\equiv\delta f_{11}+\delta f_{22}+\delta f_{12}+\delta f_{21}$ and $\delta F_2=\delta f_{11}+\delta f_{22}-\delta f_{12}-\delta f_{21}$. The solution of Eq. (A9) is

$$\Phi^{\rm ind}(q,z;\omega)=\begin{cases}-(\pi e/\epsilon_s q)\delta F_2\ e^{q(z+a)}-(\pi e/\epsilon_s q)\delta F_1\ e^{q(z-a)}, & z<-a\\ -(\pi e/\epsilon_s q)\delta F_2\ e^{-q(z+a)}-(\pi e/\epsilon_s q)\delta F_1\ e^{q(z-a)}, & -a<z<a\\ -(\pi e/\epsilon_s q)\delta F_2\ e^{-q(z+a)}-(\pi e/\epsilon_s q)\delta F_1\ e^{-q(z-a)}. & z>a.\end{cases} \tag{A10}$$

From Eqs. (26) and (A10), the matrix elements of the induced potential $\Phi_{\alpha\alpha'}(q,\omega)$ defined in Eq. (A8) are given by

$$\Phi_{11}(q,\omega) = \Phi_{22}(q,\omega) = -\frac{\pi e}{\epsilon_s q}\left(\delta f_{11} + \delta f_{22}\right)\left(1 + e^{-2qa}\right), \tag{A11a}$$

$$\Phi_{12}(q,\omega) = \Phi_{21}(q,\omega) = -\frac{\pi e}{\epsilon_s q}\left(\delta f_{12} + \delta f_{21}\right)\left(1 - e^{-2qa}\right). \tag{A11b}$$

Substituting Eq. (A7) into Eq. (A11) and setting $\varphi^{\rm ext} = 0$, we obtain the equations determining the plasmon excitation energies as

$$\left[V_1\left(\Pi_{11}^{(0)} + \Pi_{22}^{(0)}\right) - 1\right]\left(\delta f_{11} + \delta f_{22}\right) = 0\,, \tag{A12a}$$

$$\left[V_2\left(\Pi_{12}^{(0)} + \Pi_{21}^{(0)}\right) - 1\right]\left(\delta f_{12} + \delta_{21}\right) = 0\,, \tag{A12b}$$

where $V_{1,2} \equiv \pi e^2/(\varepsilon_s q)\left(1 \pm e^{-2qa}\right)$. When the first of the two equations in (29) is satisfied, from Eq. (A12b) we obtain $\delta f_{12} = -\delta f_{21}$. This solution corresponds to the case when the signs of the charge density fluctuations in each quantum well are the same [see Eq. (A10)]. Therefore, the first equation in (29) describes in-phase density fluctuations, i.e., the symmetric mode. When the second of the two equations in (29) is satisfied, from Eq. (A12a) we obtain $\delta f_{11} = -\delta f_{22}$. This is the solution when the signs of the charge density fluctuations in each quantum well are opposite. Therefore, the second equation in (29) describes out-of-phase density fluctuations, i.e., the antisymmetric mode.

* Also at The Graduate School and University Center of the City University of New York, New York, NY 10036.

[1] S. Das Sarma and A. Madhukar, Phys. Rev. B **23**, 805 (1981).
[2] P. J. Price, Physica B **117**, 750 (1983).
[3] P. M. Solomon, P. J. Price, D. J. Frank, and D. C. La Tulipe, Phys. Rev. Lett. **63**, 2508 (1989).
[4] R. Decca, A. Pinczuk, S. Das Sarma, L. N. Pfeiffer, and K. W. West, Phys. Rev. Lett. **72**, 1506 (1994).
[5] T. J. Gramila, J. P. Eisenstein, A. H. MacDonald, L. N. Pfeiffer, and K. W. West, Phys. Rev. Lett. **66**, 1216 (1991).
[6] H. C. Tso, P. Vasilopoulos, and F. M. Peeters, Phys. Rev. Lett. **68**, 2516 (1992).
[7] C. Zhang, Phys. Rev. B **49**, 2939 (1994).
[8] P. I. Tamborenea and S. Das Sarma, Phys. Rev. B **49**, 16 821 (1994); S. Das Sarma and P. I. Tamborenea, Phys. Rev. Lett. **73**, 1971 (1994).
[9] G. S. Boebinger, H. W. Jiang, L. N. Pfeiffer, and K. W. West, Phys. Rev. Lett. **64**, 1793 (1990).
[10] R. C. Ashoori, J. A. Lebens, N. F. Bigelow, and R. H. Silsbee, Phys. Rev. Lett. **64**, 681 (1990).
[11] R. C. Ashoori, J. A. Lebens, N. F. Bigelow, and R. H. Silsbee, Phys. Rev. B **48**, 4616 (1993).
[12] A. H. MacDonald, Surf. Sci. **229**, 1 (1990); L. Zheng and A. H. MacDonald, Phys. Rev. B **47**, 10 619 (1993).
[13] A. H. MacDonald and S.-C. Zhang, Phys. Rev. B **49**, 17 208 (1994).
[14] J. P. Eisenstein, L. N. Pfeiffer, and K. W. West, Phys. Rev. Lett. **69**, 3804 (1992).
[15] S. He, P. M. Platzman, and B. I. Halperin, Phys. Rev. Lett. **71**, 777 (1993).
[16] P. Johansson and J. M. Kinaret, Phys. Rev. Lett. **71**, 1435 (1993).
[17] A. L. Efros and F. G. Pikus, Phys. Rev. B **48**, 14 694 (1993).
[18] S.-R. E. Yang and A. H. MacDonald, Phys. Rev. Lett. **70**, 4110 (1993).
[19] Y. Hatsugai, P.-A. Bares, and X. G. Wen, Phys. Rev. Lett. **71**, 424 (1993).
[20] G. R. Aĭzin and G. Gumbs (unpublished).
[21] K. Brown and M. Pepper (unpublished).
[22] P. C. Martin and J. Schwinger, Phys. Rev. **115**, 1342 (1959).
[23] M. O. Manasreh and J. P. Loehr, in *Semiconductor Quantum Wells and Superlattices for Long Wavelength Infrared Detection*, edited by M. O. Manasreh (Artech House, Norwood, MA, 1993), Chap. 2.
[24] P. von Allmen, M. Berz, F. K. Reinhart, and G. Harbeke, Superlatt. Microstruct. **5**, 259 (1989).
[25] P. von Allmen, M. Berz, G. Petrocelli, F. K. Reinhart, and G. Harbeke, Semicond. Sci. Technol. **3**, 1211 (1988).
[26] U. Ekenberg, Phys. Rev. B **36**, 6152 (1987).
[27] G. D. Mahan, *Many-Particle Physics* (Plenum, New York, 1990), p. 263.
[28] G. Gumbs, D. Huang, Y. Yin, H. Qiang, D. Yan, F. H. Pollak, and T. F. Noble, Phys. Rev. B **48**, 18 328 (1993).
[29] K. Esfarjani, H. R. Glyde, and V. Sa-yakanit, Phys. Rev. B **41**, 1042 (1990).
[30] K. Bandara, D. D. Coon, O. Byungsung, Y. F. Lin, and M. H. Francombe, Appl. Phys. Lett. **53**, 1931 (1988).
[31] W. H. Press, B. P. Flannery, S. A. Teukolsky, and W. T. Vetterling, *Numerical Recipes* (Cambridge, New York, 1986), Chap. 4.
[32] J. K. Jain and S. Das Sarma, Phys. Rev. B **36**, 5949 (1987).